GU J Sci, Part A, 5(1): 1-15 (2018)

Gazi University

Journal of Science

PART A: ENGINEERING AND INNOVATION

http://dergipark.gov.tr/gujsa

3-D Analytical Treatment of Base Isolation For Mechanical Testing Systems

Mehmet ŞAHİN[1,*]

[1]*TAI, Fethiye Mahallesi, Havacılık Bulvarı, No:17, 06980, Kahramankazan, Ankara, TURKEY*

Article Info

Received: 27/08/2017
Accepted: 08/12/2017

Keywords

Vibration isolation,
Rigid-body motion,
Eigen-analysis,
Sine-sweep test

Abstract

A mathematical model for dynamic analysis of vibration isolation systems is presented. The model is based on small deformation mechanics of 3-D rigid body with 6-DOF and supported by flexible structural members. The mass, static stiffness and damping matrices for the system are derived. Eigen-analysis using the presented model and solution method are applied to a real spacecraft vibration test system with base isolation. A finite element model of the system is also developed. The results of the proposed math model, FE model and test results of a real vibration testing system are compared. The math model solution results agree well with the FEM model and actual test results. The model can be used in the design of the engineering structures with base isolation such as vibration and acoustic test systems, large static and dynamic testing systems, buildings etc.

1. INTRODUCTION

There are wide application areas of base isolation systems for large engineering structures and systems such as engines, turbines, mechanical testing systems, buildings, bridges, etc. One application area of huge massive base isolations systems is spacecraft mechanical testing systems. For example, acoustic and vibration testing systems are among the major mechanical testing systems in the aerospace industry. These systems require base isolations to reduce and isolate the vibration caused by these systems since the isolation system decouples the structure from its foundation and adds flexibility. The acoustic testing systems have base isolations to isolate the vibration and noise caused by the acoustic noises in reverberation chambers during the acoustic tests. Similarly, vibration caused by the vibration shakers in vibration testing systems are isolated by the base isolation systems. The testing systems are massive structures, for example, the mass of an actual vibration testing system considered in this study is around 350 metric tons and the mass of an actual acoustic testing system is over 1000 metric tons [1]. Three-types of vibration tests are done on these types of vibration testing systems. These are sine, random and shock tests. The types and levels of these tests determine the capacity, size, supporting and geometry of the shaker and base isolation of the test systems.

1.1. The analytical models

Analytical math models for design of base isolation systems can save time and can precisely determine structural design parameters such size, capacity, volume, mass, number of structural members etc. The matrix form or the direct equilibrium concepts are two common approaches to formulate the math models of the base isolation systems. In these methods, the main massive body is assumed to be rigid and having 6- degree of freedom with 3 translations and 3 rotations. The simplest approach to design of base isolation system with relatively small eccentricities is to assume that the system behaves in uncoupled modes of a six degree-of-freedom of system. In that case, each of six degree of freedom becomes independent single-degree-of-freedom (SDOF) systems and the required stiffness for each direction is obtained for given isolation level and excitation frequency. However, coupled behavior of the complex systems is unavoidable

*Corresponding author, e-mail: drmsahin@outlook.com

due to unsymmetrical and uneven mass and stiffness distributions, manufacturing, erection, and alignment errors during construction etc. The distance between the mass and stiffness centers causes eccentricities and results in coupled behavior between the translational and rotational degrees of freedoms. The coupled behavior requires more detailed math models and solution methods. Although the finite element method makes the realistic model more possible than the analytical models, it may not be practical to create a finite element model without having initial design. However, the analytical models help designers to obtain better initial parameters for the design and modeling of the finite element model. The main concern in the preliminary design of the system is to find eigen-frequencies and the rigid body modes of the vibration isolation system. The massive isolation block is an elastic structure having much larger elastic stiffness than the supporting springs, thus its eigen-frequencies are much larger than the rigid mode eigen-frequencies. Thus, elastic eigen-modes is not considered in the preliminary design of the system.

There are many studies in regards to the formulation of dynamic analysis of isolation systems. In these studies, the matrix form or direct form of governing equilibrium equations in 3-D are used for rigid body dynamics of the system. Himelblau and Rubin explicitly present the Newton-Euler dynamic equilibrium equations and examine one- and two-plane symmetries with orthogonal resilient supports cases [2]. Matrix form of the equation of motion for vibration-isolation systems is given by Smollen [3]. He obtained the translational, rotational, rotational-translational and translational-rotational sub-matrices separately to form static stiffness matrix by using matrix form of the position vector **r**. One and two-stage vibration isolation systems are examined by Moore [4]. The two-stage is defined as two rigid bodies supported by springs one on the top of the other body like in two-story buildings. Jun et.al give formulation of the static stiffness of the vehicle mounts using elastically supported rigid body [5]. They also calculate different dynamic stiffness matrices of the mounts by using different vibration tests. Then, the results of the eigen-analysis using different stiffness matrices obtained by the static formulation, experimentally obtained dynamic stiffness, impact hummer and operational modal analysis tests are compared. Iwan uses an equivalent linear system method to linearize the spring-limiter type nonlinear isolators of the isolation system [6]. In his study, different translational and rotational degree of freedom are used. The principal axes of inertia are selected as rotational degrees of freedom of the system while translational directions are selected according to the coordinate system directions. This assumption results in diagonal inertia matrix in the system. Lagrangian dynamics is also used by Madsen [7] to formulate and obtain the governing equations of motion and the eigenvalue problem of the system is solved. Researchers also examined non-linear behavior of passive vibration isolation systems. The nonlinearities originating from large deformation, stiffness and geometric nonlinearities can be found in different fields of engineering. The study by Ibrahim summarizes types of nonlinear vibration isolators and past studies on these isolators [8].

In this study, the static stiffness matrix based on the small displacement of rigid body supported by elastic, axially stiff springs is derived using vector algebra [9]. Small displacement of a rigid body is separated into translation and rotation parts in vector forms. The displacement induced forces on the springs attached to the point on the moving rigid body is derived. Then the static stiffness matrix relating force-displacement relation is obtained. The origin of the coordinate system for governing dynamic equilibrium equation in matrix form is taken as the center of mass of system. The rotational directions are taken around the inertial reference coordinate system. The mass and stiffness matrices based on the chosen coordinate system becomes non-diagonal for arbitrarily shaped isolation system. The dynamic equilibrium equation and the equation for eigen-analysis based on derived the stiffness and mass matrices are given. The derived equations are applied to a real isolation system where the method results are compared with the actual test results. The real test results are obtained from the vibration testing facility acceptance tests. The test is conducted to ensure that rigid body frequencies of the testing system are within the theoretical design frequencies. Finite element model is also developed by using a commercial finite element software. The results of the analytical math model, finite element model and the interpolated test results are compared. The small differences between the models and test results are examined and conclusions are drawn.

2. THEORETICAL MODEL ANALYSIS OF BASE ISOLATION SYSTEMS

2.1. Theoretical Model

Consider an arbitrarily shaped rigid body attached to the rigid ground via mutually perpendicular elastic springs with dampers at some connection points. Let's define a Cartesian coordinate system $o-xyz$ as a fixed inertial coordinate system and select its origin as the center of mass of the whole system including the block and payload on it. The model and coordinate systems are shown in the Figure 1. The ground plane is selected as *x-y* plane and consequently, the *z*-axis becomes perpendicular to the ground plane. The rigid body motion is represented with a 6-DOF system which are three translations along and three rotations around three perpendicular directions. They also represent generalized coordinates in dynamic and static analysis of rigid bodies. The rotations around the *x* and *y* axes are usually termed rocking and rotation around the *z* axis is named yawing. The local body moving coordinate system coincides with the inertial coordinate system when the system is at rest. The system has *N*-number of supports points and is subjected to a dynamic load causing small translations and rotations.

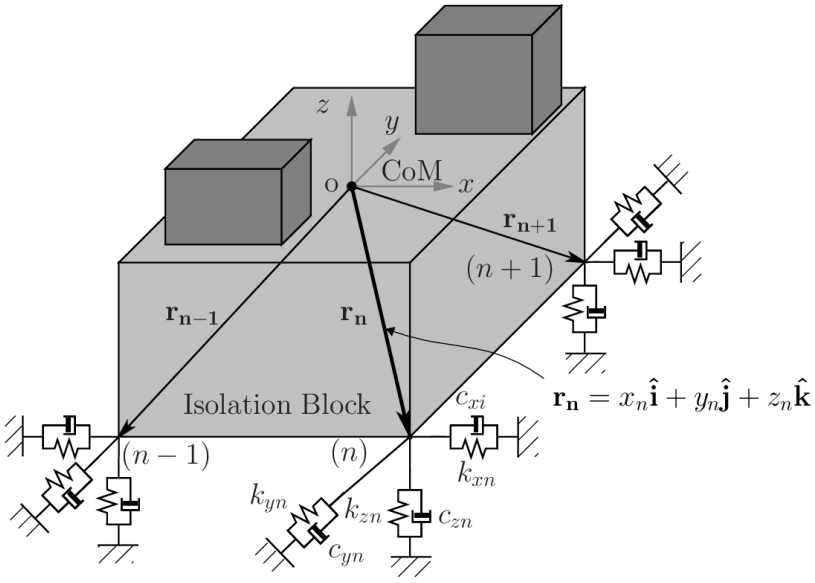

Figure 1. *Resiliently supported rigid body model at rest*

The position of a support at the point-*n* on the body can be represented by a position vector $\mathbf{r}_n = x_n\mathbf{i} + y_n\mathbf{j} + z_n\mathbf{k}$ with respect to the origin at rest. When the center of mass is taken as origin, displacement of the point-*n* $\left(\mathbf{d}_n = d_{xn}\,\hat{\mathbf{i}} + d_{yn}\,\hat{\mathbf{j}} + d_{zn}\,\hat{\mathbf{k}}\right)$, is due to rigid body translation $\left(\mathbf{u} = u_x\,\hat{\mathbf{i}} + u_y\,\hat{\mathbf{j}} + u_z\,\hat{\mathbf{k}}\right)$ and rotation $\boldsymbol{\theta}\left(\boldsymbol{\theta} = \theta_x\,\hat{\mathbf{i}} + \theta_y\,\hat{\mathbf{j}} + \theta_z\,\hat{\mathbf{k}}\right)$ of the body around the center of mass. Total displacement of the point-*n* can be written in matrix form of

$$\mathbf{d}_n \;=\; \mathbf{u} + \boldsymbol{\theta} \times \mathbf{r}_n = \mathbf{I}\mathbf{u} + skew(\mathbf{r}_n)^T\boldsymbol{\theta} = \mathbf{I}\mathbf{u} - skew(\mathbf{r}_n)\boldsymbol{\theta} = \mathbf{I}\mathbf{u} - \mathbf{R}_n\boldsymbol{\theta} \tag{1}$$

where $\mathbf{I}$ is identity matrix and $skew(\mathbf{r}_n) = \mathbf{R}_n = -\mathbf{R}_n^T$ is skew-symmetric matrix representation of the position vector $\mathbf{r}_n$ [9]. Explicit form of the equation becomes

$$\mathbf{d}_n = \begin{bmatrix} d_{xi} \\ d_{yi} \\ d_{zi} \end{bmatrix} = \begin{bmatrix} 1 & 0 & 0 \\ 0 & 1 & 0 \\ 0 & 0 & 1 \end{bmatrix} \begin{bmatrix} u_x \\ u_y \\ u_z \end{bmatrix} - \begin{bmatrix} 0 & -z_n & y_n \\ z_n & 0 & -x_n \\ -y_n & x_n & 0 \end{bmatrix} \begin{bmatrix} \theta_x \\ \theta_y \\ \theta_z \end{bmatrix} \tag{2}$$

The right-hand rule is applied and the counterclockwise rotation direction is taken as positive. The total displacement vector $\mathbf{d}_i$ for the point-i can be related to the generalized coordinates $\mathbf{q}$ of the system via $\mathbf{B}_n$ position matrix as

$$\mathbf{d}_n \quad = \quad \mathbf{B}_n\mathbf{q} = [\mathbf{I} \quad | \quad \mathbf{R_n^T}]\mathbf{q} = \begin{bmatrix} 1 & 0 & 0 & 0 & z_n & -y_n \\ 0 & 1 & 0 & -z_n & 0 & x_n \\ 0 & 0 & 1 & y_n & -x_n & 0 \end{bmatrix} \begin{bmatrix} \mathbf{u} \\ - \\ \boldsymbol{\theta} \end{bmatrix} \tag{3}$$

where $\mathbf{q}^T = [\mathbf{u} \quad | \quad \boldsymbol{\theta}]^T = [u_x \quad u_v \quad u_z \quad \theta_x \quad \theta_y \quad \theta_z]^T$is global displacement vector representing generalized coordinates of the system. The linear elastic stiffness matrix for the spring system at the point-*n* in local coordinate system is shown as $\mathbf{K'}_n$ and transformed from the spring local coordinate system (x', y', z') to the global coordinate system (x, y, z) by the transformation equation $\mathbf{K}_n = \mathbf{Q}_n^T\mathbf{K'}_n\mathbf{Q}_n$. The $\mathbf{Q}_n$ is transformation matrix from local coordinate system to global coordinate system for the nth spring system. After the transformation, the symmetric stiffness matrix in global coordinate system can be written as

$$\mathbf{K}_n = \mathbf{Q}_n^T\mathbf{K'}_n\mathbf{Q}_n = \begin{bmatrix} k_{11} & k_{12} & k_{13} \\ k_{21} & k_{22} & k_{23} \\ k_{31} & k_{32} & k_{33} \end{bmatrix}_n \tag{4}$$

The springs are assumed to be composed of axial spring elements and rotational stiffness of them are assumed to be relatively small and they are neglected. The elastic static force developed on the springs at the point-*n* is product of the stiffness matrix $\mathbf{K}_n$, and the displacement of the point-*n* $\mathbf{d}_n$.

$$\mathbf{f}_n \quad = \mathbf{K}_n\mathbf{d}_n \quad = \mathbf{K}_n\mathbf{B}_n\mathbf{q} = [\mathbf{K}_n\mathbf{I} \quad \mathbf{K}_n\mathbf{R}_n^T]\mathbf{q} = [\mathbf{K}_{tt,n} \quad \mathbf{K}_{tr,n}]\mathbf{q} \tag{5}$$

and can be expressed in explicit form as

$$\mathbf{f}_n = \begin{bmatrix} f_{xn} \\ f_{yn} \\ f_{zn} \end{bmatrix} = \begin{bmatrix} k_{11,n} & k_{12,n} & k_{13,n} & (y_n k_{13,n} - z_n k_{12,n}) & (z_n k_{11,n} - x_n k_{13,n}) & (x_n k_{12,n} - y_n k_{11}) \\ k_{21,n} & k_{22,n} & k_{23,n} & (y_n k_{23,n} - z_n k_{22,n}) & (z_n k_{21,n} - x_n k_{23,n}) & (x_n k_{22,n} - y_n k_{21,n}) \\ k_{31,n} & k_{32,n} & k_{33,n} & (y_n k_{33,n} - z_n k_{23,n}) & (z_n k_{13,n} - x_n k_{33,n}) & (x_n k_{23,n} - y_n k_{13,n}) \end{bmatrix} \mathbf{q} \tag{6}$$

where the sub-stiffness matrices $\mathbf{K}_{tt.n} = \mathbf{K}_n\mathbf{I}$ and $\mathbf{K}_{tr.n} = \mathbf{K}_n\mathbf{R}_n^T$ correspond to the translation and rotation-translation coupling for the spring system at the point-*n* respectively. Note that the first three columns of the stiffness matrix in the Eq. 6 is $\mathbf{K}_{tt.n} = \mathbf{K}_n\mathbf{I}$ and the last three columns corresponds to $\mathbf{K}_{tr.n} = \mathbf{K}_n\mathbf{R}_n^T$. Similarly, under small deformation assumption, the moment $\mathbf{t}_n$ about the mass center is the cross product of the position vector $\mathbf{r}_n$ and the force $\mathbf{f}_n$ on the point-n linear elastic springs can be written as

$$\mathbf{t}_n = \begin{bmatrix} t_{xn} \\ t_{yn} \\ t_{zn} \end{bmatrix} = \mathbf{r}_n \times \mathbf{f}_n = \mathbf{r}_n \times (\mathbf{K}_n\mathbf{d}) = [\mathbf{K}_{rt,n} \quad \mathbf{K}_{rr,n}]\mathbf{q} = \mathbf{R}_n\mathbf{K}_n\mathbf{B}_n\mathbf{q} \tag{7}$$

where $\mathbf{K}_{rt,n}$ and $\mathbf{K}_{rr,n}$ are sub-stiffness matrices of the *n*-th support for the translation-rotation coupling and the rotation respectively. They are evaluated and given as

$$\mathbf{K}_{rt,n} = \mathbf{R}_n\mathbf{K}_n\mathbf{I} = \begin{bmatrix} (y_n k_{13,n} - z_n k_{12,n}) & (y_n k_{23,n} - z_n k_{22,n}) & (y_n k_{33} - z_n k_{23,n}) \\ (z_n k_{11,n} - x_n k_{13,n}) & (z_n k_{12,n} - x_n k_{23,n}) & (z_n k_{13} - x_n k_{33,n}) \\ (x_n k_{21,n} - y_n k_{11,n}) & (x_n k_{22,n} - y_n k_{12,n}) & (x_n k_{23} - y_n k_{13,n}) \end{bmatrix} \tag{8}$$

and

$$\mathbf{K}_{rr,n} = \begin{bmatrix} y_n^2 k_{33,n} + z_n^2 k_{22,n} - 2z_n y_n k_{23,n} & z_n\left(x_n k_{23,n} + y_n k_{31,n} - z_n k_{21,n}\right) - x_n y_n k_{33,n} & y_n \\ z_n\left(x_n k_{23,n} + y_n k_{13,n} - z_n k_{12,n}\right) - x_n y_n k_{33,n} & x_n^2 k_{33,n} + z_n^2 k_{11,n} - 2x_n z_n k_{13,n} & x_n \\ y_n\left(x_n k_{23,n} - y_n k_{13,n} + z_n k_{12,n}\right) - x_n z_n k_{22,n} & x_n\left(y_n k_{13,n} + z_n k_{21,n} - x_n k_{23,n}\right) - y_n z_n k_{11,n} & x_n \end{bmatrix} \quad (9$$

Note that the $\mathbf{K}_{rt,n} = \mathbf{K}_{tr,n}^T$ because of symmetry of the stiffness matrices. Now, force-displacement and moment-rotation relations can be combined in a single matrix

$$\mathbf{F}_n = \begin{bmatrix} \mathbf{f}_n \\ - \\ \mathbf{t}_n \end{bmatrix} = \mathbf{K}_{cn}\mathbf{q} = \begin{bmatrix} \mathbf{K}_{tt,n} & \vert & \mathbf{K}_{rt,n} \\ - & - & - \\ \mathbf{K}_{tr,n} & \vert & \mathbf{K}_{rr,n} \end{bmatrix}\mathbf{q} \quad (10)$$

or shortly $\mathbf{F}_\mathrm{n} = \mathbf{K}_\mathrm{n}\mathbf{q}$ where $\mathbf{K}_\mathrm{n}$ static stiffness matrix due to the spring system at the point-n and $\mathbf{F}_n$ is the force vector due to displacement of the elastic spring system located at that point. If more than one spring systems, say N, having different stiffness values are attached to the rigid block, the global stiffness matrix $\mathbf{K}_G$ is obtained by summation of all spring system stiffness values.

$$\mathbf{F}_G = \sum_{n=1}^{N}\mathbf{F}_n = \begin{bmatrix} \mathbf{f}_G \\ - \\ \mathbf{t_G} \end{bmatrix} = \begin{bmatrix} \sum_{n=1}^{N}\mathbf{f}_n \\ - \\ \sum_{n=1}^{N}\mathbf{t}_n \end{bmatrix} = \mathbf{K}_G\mathbf{q} = \left(\sum_{n=1}^{N}\mathbf{K}_{cn}\right)\mathbf{q} = \left(\sum_{n=1}^{N}\begin{bmatrix} \mathbf{K}_{tt,n} & \vert & \mathbf{K}_{rt,n} \\ - & - & - \\ \mathbf{K}_{tr,n} & \vert & \mathbf{K}_{rr,n} \end{bmatrix}\right)\mathbf{q} \quad (11)$$

$$\mathbf{F}_G = \begin{bmatrix} \mathbf{f}_G \\ - \\ \mathbf{t_G} \end{bmatrix} = \begin{bmatrix} \mathbf{K}_{tt} & \vert & \mathbf{K}_{rt} \\ - & - & - \\ \mathbf{K}_{tr} & \vert & \mathbf{K}_{rr} \end{bmatrix}\mathbf{q} = \mathbf{K}_G\mathbf{q} \quad (12)$$

Note that $\mathbf{f}_G$ and $\mathbf{t}_G$ are global static force and moment vectors respectively. The same analogy can be used to obtain damping matrix as $\mathbf{F}_d = \mathbf{C}\mathbf{q}$. Recall that the formulation derived above is based on the assumption that the mass center is the origin of the coordinate system. The mass matrix is independent of location of the supports, if the mass of the springs is small and ignored, and it becomes

$$\mathbf{M}_G = \begin{bmatrix} \mathbf{M} & \vert & \mathbf{0} \\ - & - & - \\ \mathbf{0} & \vert & \mathbf{J} \end{bmatrix} = \begin{bmatrix} M & 0 & 0 & 0 & 0 & 0 \\ 0 & M & 0 & 0 & 0 & 0 \\ 0 & 0 & M & 0 & 0 & 0 \\ 0 & 0 & 0 & J_{xx} & J_{xy} & J_{xz} \\ 0 & 0 & 0 & J_{xy} & J_{yy} & J_{yz} \\ 0 & 0 & 0 & J_{xz} & J_{yz} & J_{zz} \end{bmatrix} \quad (13)$$

where **M** submatrix is mass matrix for the translation and **J** is the inertia matrix for the angular movement. The zero submatrices are due to the fact that the center of mass is taken as origin. If the structure is symmetric in mass distribution, then the product inertia values J_{xy}, J_{xz}, and J_{yz} become zero and mass matrix becomes diagonal. More general dynamic equilibrium equation including support excitation, such as earthquake, and dynamic loading caused by the equipment on the block can be written as

$$\mathbf{M}_G\ddot{\mathbf{q}}(t) + \mathbf{C}_G\dot{\mathbf{q}}(t) + \mathbf{K}_G\mathbf{q}(t) = -\mathbf{M}_G\ddot{\mathbf{q}}_g(t) + \mathbf{F}_e(t) \quad (14)$$

where the $\ddot{\mathbf{q}}_g$ support (or ground) excitation vector which have all components of ground accelerations including both translational and rotational components and it is given as

$$\ddot{\mathbf{q}}_{\mathbf{g}} = \left[\ddot{\mathbf{u}}_{\mathbf{g}}(t) \quad \ddot{\boldsymbol{\theta}}_{\mathbf{g}}(t)\right]^{\boldsymbol{T}} = \left[\ddot{\mathrm{u}}_{\mathrm{g}}(\mathrm{t}) \quad \ddot{\mathrm{v}}_{\mathrm{g}}(\mathrm{t}) \quad \ddot{\mathrm{w}}_{\mathrm{g}}(\mathrm{t}) \quad \ddot{\theta}_{\mathrm{g,x}}(\mathrm{t}) \quad \ddot{\theta}_{\mathrm{g,y}}(\mathrm{t}) \quad \ddot{\theta}_{\mathrm{g,z}}(\mathrm{t})\right]^{\boldsymbol{T}} \tag{15}$$

And external force vector $\mathbf{F}_e$ is given as $\mathbf{F}_e = [F_x \quad F_y \quad F_z \quad | \quad T_{g,x} \quad T_{g,y} \quad T_{g,z}]^T$. Note that both components of support excitation $\ddot{\mathbf{q}}_g(t)$ and the force vector $\mathbf{F}_e(t)$ are functions of time.

2.2. Special cases

Symmetry in mass distribution, support locations and the spring systems at the supports reduce the complexity of the governing equations. Some symmetry cases will be examined in detail.

2.2.1. No-coupled springs system at the supporting points

If the system of three springs at all support points are mutually perpendicular to each other and their axes are parallel to the axes of the reference coordinate system, then the off-diagonal terms of the stiffness matrix vanish i.e., $k_{12} = k_{23} = k_{13} = 0$. Then, the stiffness matrix of the system becomes

$$\mathbf{K}_G = \sum_{n=1}^{N} \begin{bmatrix} k_{11,n} & 0 & 0 & 0 & z_n k_{11,n} & -y_n k_{11,n} \\ 0 & k_{22,n} & 0 & -z_n k_{22,n} & 0 & x_n k_{22,n} \\ 0 & 0 & k_{33,n} & y_n k_{33,n} & -x_n k_{33,n} & 0 \\ 0 & -z_n k_{22,n} & y_n k_{33,n} & y_n^2 k_{33,n} + z_n^2 k_{22,n} & -x_n y_n k_{33,n} & -x_n z_n k_{22,n} \\ z_n k_{11,n} & 0 & -x_n k_{33,n} & -x_n y_n k_{33,n} & x_n^2 k_{33,n} + z_n^2 k_{11,n} & -y_n z_n k_{11,n} \\ -y_n k_{11,n} & x_n k_{22,n} & 0 & -x_n z_n k_{22,n} & -y_n z_n k_{11,n} & x_n^2 k_{22,n} + y_n^2 k_{11} \end{bmatrix} \tag{16}$$

2.2.2. Geometric symmetry with respect to one axis (x-axis)

If all springs have the same stiffness in lateral x- and y-axes and are symmetrically placed with respect to the global y-axis. The stiffness matrix becomes

$$\mathbf{K}_G = \begin{bmatrix} K_{11} & 0 & 0 & 0 & e_{zx}K_{11} & 0 \\ 0 & K_{22} & 0 & -e_{zy}K_{22} & 0 & e_{xy}K_{22} \\ 0 & 0 & K_{33} & 0 & -e_{xz}K_{33} & 0 \\ 0 & -e_{zy}K_{22} & 0 & y_n^2 k_{33,n} + z_n^2 k_{22,n} & -x_n y_n k_{33,n} & -x_n z_n k_{22,n} \\ e_{zx}K_{11} & 0 & -e_{xz}K_{33} & -x_n y_n k_{33,n} & x_n^2 k_{33,n} + z_n^2 k_{11,n} & -y_n z_n k_{11,n} \\ 0 & e_{xy}K_{22} & 0 & -x_n z_n k_{22,n} & -y_n z_n k_{11,n} & x_n^2 k_{22,n} + y_n^2 k_{11,n} \end{bmatrix} \tag{17}$$

where

$$K_{11} = \sum_{n=1}^{N} k_{11,n} \qquad K_{22} = \sum_{n=1}^{N} k_{22,n} \qquad K_{33} = \sum_{n=1}^{N} k_{33,n}$$

$$e_{zx} = \frac{\sum_{n=1}^{N} k_{11,n}\, z_n}{K_{11}} \qquad e_{xz} = \frac{\sum_{n=1}^{N} k_{33,n}\, x_n}{K_{33}}$$

$$e_{yx} = \frac{\sum_{n=1}^{N} k_{11,n}\, y_n}{K_{11}} \qquad e_{xy} = \frac{\sum_{n=1}^{N} k_{22,n}\, x_n}{K_{22}}$$

$$e_{zy} = \frac{\sum_{n=1}^{N} k_{22,n}\, z_n}{K_{22}} \qquad e_{yz} = \frac{\sum_{n=1}^{N} k_{33,n}\, y_n}{K_{33}}$$

2.2.3. Geometric symmetry with respect to two axes (x-and y-axes)

In the case of the geometric symmetry of the support points with respect to both x and y-axes and the same stiffness in global x and y-axes ($K_{11} = K_{22} = K$) result in the following stiffness matrix.

$$\mathbf{K}_G = K \sum_{n=1}^{N} \begin{bmatrix} 1 & 0 & 0 & 0 & z_n & 0 \\ 0 & 1 & 0 & -z_n & 0 & 0 \\ 0 & 0 & \frac{K_{33}}{K} & 0 & 0 & 0 \\ 0 & -z_n & 0 & y_n^2 \frac{K_{33}}{K} + z_n^2 & 0 & 0 \\ z_n & 0 & 0 & 0 & x_n^2 \frac{K_{33}}{K} + z_n^2 & 0 \\ 0 & 0 & 0 & 0 & 0 & x_n^2 + y_n^2 \end{bmatrix} \tag{18}$$

The model discussed previously can be used to model and analysis different engineering structures which resembles to resiliently mounted quasi-rigid engineering systems. One example is one story building supported by columns (Figure 2). The columns behave as springs acting in horizontal and vertical directions, but the story plane acts as rigid plane with three degree of freedom rotations and three translations in x, y, and z directions.

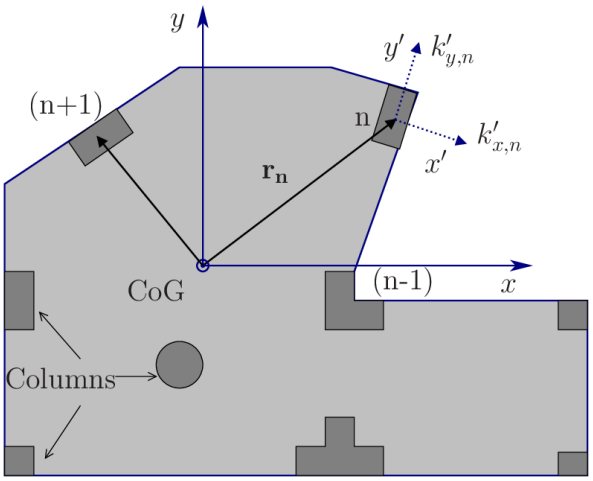

Figure 2. *One-story building supported by columns*

Although there are numerous aplication areas in different fields of engineering, previously mentioned models are more commonly used in structural systems.

3. Application in Eigen-analysis

The stiffness matrix constitutes the force-displacement relation and is used in static and dynamic analysis of engineering structures. For example, for undamped free vibration analysis, the damping can be ignored and the governing equation be written as

$$\mathbf{M}\ddot{\mathbf{q}}(t) + \mathbf{K}\mathbf{q}(t) = \mathbf{0} \tag{19}$$

Using the separation of variables method for $\mathbf{q} = \mathbf{Q}e^{-i\omega t}$, the equation for free-vibration analysis reduces to

$$[\mathbf{K} - \omega^2\mathbf{M}]\mathbf{Q} == \mathbf{0} \tag{20}$$

Where $\mathbf{Q}^T = [U_x, U_y, U_z, \Theta_x, \Theta_y, \Theta_z]$ is mode displacement vector and ω is the eigen-frequency. This is eigen-analysis equation for the system. The system is solved and its 6 eigen-values and eigen-modes are obtained. For asymmetrically supported body and unevenly distributed mass, eccentricities in one, two or three axes can occur depending upon the mass and stiffness distributions. For full symmetry in all axes, the stiffness matrix becomes diagonal and greatly simplifies the eigen-analysis. For both symmetric mass and stiffness distribution, mass and stiffness matrices become symmetric and diagonal and 6 independent equations are obtained for eigen-analysis.

The vibration isolation system for the application is an isolation system of the actual spacecraft vibration testing system specifically designed for large spacecraft up-to 5 tons. The shakers for the system are large and massive machines and require effective isolated base systems. Test limits of the system impose that the fundamental frequency must be smaller than 3 Hz and vibration isolation must be lower than a certain level. The fundamental frequency requirement comes from the fact that the vibration testing system has to be capable of executing sine-sweep tests from 5 Hz to 2000 Hz. The second requirement is that the vibration isolation level at the point located 1 meter away from the testing system must be larger than -20 decibel. The total mass of the vibration testing system is around 350,000 kg. The inertia block of the isolation system has a shape of a T-section and is made of reinforced concrete. Details of the block is shown on the *Figure 3*. The length and height of the block is 9 and 4 meter respectively. The mass of the block is 293 tons. The isolation block is supported by 20 equivalent spring systems, except 4 of them with additional viscous dampers, located by pairs along the length of the seismic block i.e. there are 10 lines of spring systems and each line has symmetric 2 spring systems. Each spring system has an assembly of 10 springs placed in line by pair or circular pattern (see the *Figure 4*).

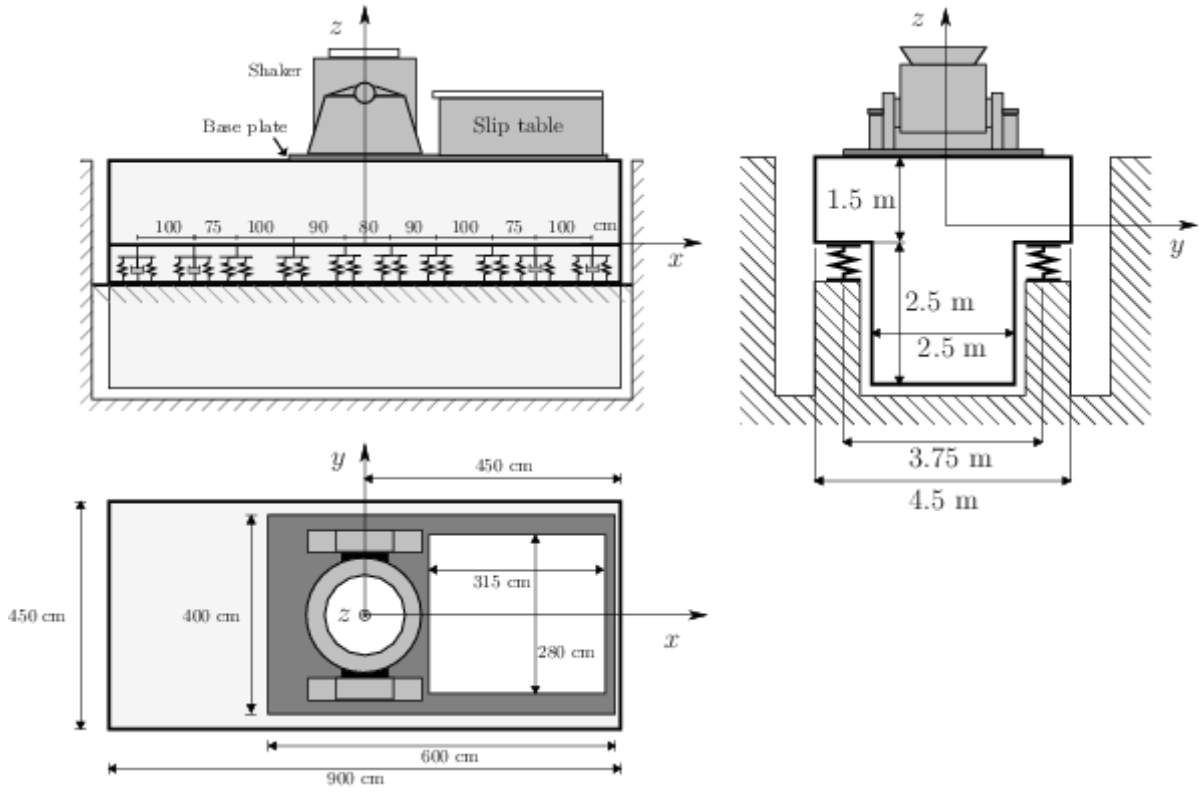

a) Side- and top-view

b) Cross-section

Figure 3. *Vibration test system*

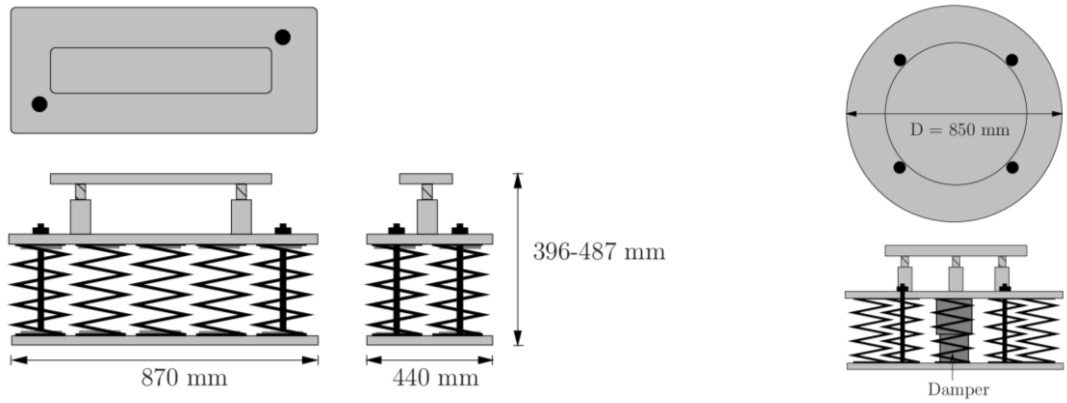

a) Without damper b) With damper

Figure 4. *Spring systems at the supports*

Figure 5. *The vibration testing system with base isolation [1]*

Figure 6. *A typical spring system at the supports [10]*

The spring systems with centrally located dampers are placed around each corner of the block. The stiffness values of each spring system in horizontal and vertical directions are 2470 N/mm and 1350 N/mm respectively [10]. The masses of the spring systems without and with dampers are 230 and 327 kg respectively. The total mass of the springs around 5000 kg and be neglected both in math and the finite element model since their mass are is less than 1.5 percent of the total mass.

The payload on the block consists of the base plate, shaker and horizontal slip table. The heaviest part of the payload is shaker and it is exactly located at the middle of the block so that minimize eccentricity. On the other hand, the slip table, which have relatively smaller mass than the shaker, is located on the negative *x*-side of the block which causes relatively small eccentricity in the *x*-direction. Distance between the mass and stiffness center in vertical direction is also small because the mass center is around the level of the springs and this distance cause a small eccentricity too. Thus, the system has relatively small eccentricities both in *x* and *z* directions causing coupled behavior.

3.1. Eigen analysis solution

The math model of the actual test system is based on the method described in the previous sections. The coordinates of the support locations and stiffness of the springs at each direction is substituted into the related equations and mass and static stiffness matrices of the system are obtained respectively as

$$M = \begin{bmatrix} 350025 & 0 & 0 & 0 & 0 & 0 \\ 0 & 350025 & 0 & 0 & 0 & 0 \\ 0 & 0 & 350025 & 0 & 0 & 0 \\ 0 & 0 & 0 & 1036398 & 0 & -171327.6 \\ 0 & 0 & 0 & 0 & 2903241 & 0 \\ 0 & 0 & 0 & -171327.7 & 0 & 2592313 \end{bmatrix} \tag{21}$$

$$K = 10^6 \begin{bmatrix} 48.6 & 0 & 0 & 0 & 8.518 & -0.522 \\ 0 & 48.6 & 0 & -8.518 & 0 & 12.213 \\ 0 & 0 & 27.0 & 0.29 & -6.785 & 0 \\ 0 & -8.518 & 0.29 & 96.649 & 0.496 & -2.141 \\ 8.518 & 0 & -6.785 & 0.496 & 184.619 & -0.092 \\ -0.522 & 12.213 & 0 & -2.141 & -0.092 & 500.908 \end{bmatrix} \tag{22}$$

Mass and length units are taken as kg and meter respectively. The stiffness matrix is obtained by summation of the stiffness values of 20 spring systems and their coordinates. It is assumed that the springs are connected to the block point-wise. The rotational stiffness of the spring systems is neglected because of their smaller stiffness as compared to translational stiffness. The rotational stiffness of the 10-spring system is approximately calculated as one-tenth of the lateral stiffness of the spring system. Thus, for the sake of simplification, the rotational stiffness is neglected both in analytical math and finite element models. The total mass and mass moment of inertia of the system is calculated. Because of accidental placement of springs, there is also an eccentricity in y-direction.

3.2. Finite element model

A detailed FE model is developed to compare its results with the analytic math model and actual test results. The reinforced concrete isolation block is assumed to be linear elastic homogeneous material and the shaker and slip table are assumed to be highly stiff bodies as compared to the block. The shaker and table are modeled as homogeneous rectangular prism having the same actual masses. The springs have stiffness values in three mutual directions and springs with dampers are only located at each corner of the block. The first three fundamental frequencies and mode shapes are shown on the
Figure 7 The mode shapes of the math model and the finite element agree well. The first and second modes look like rocking modes around *x* and *y*-axes and the sixth mode is yawing modes. The third are fourth modes are rocking modes. Note that contours on the modes shows the displacement paths of the rotational motion. The finer meshes slightly improves the eigen-frequencies and moderate meshing is applied to the model. This is due to much larger stiffness of the block as compared to the springs. The block behaves as quasi-rigid body in the finite model and finer mesh effect insignificantly.

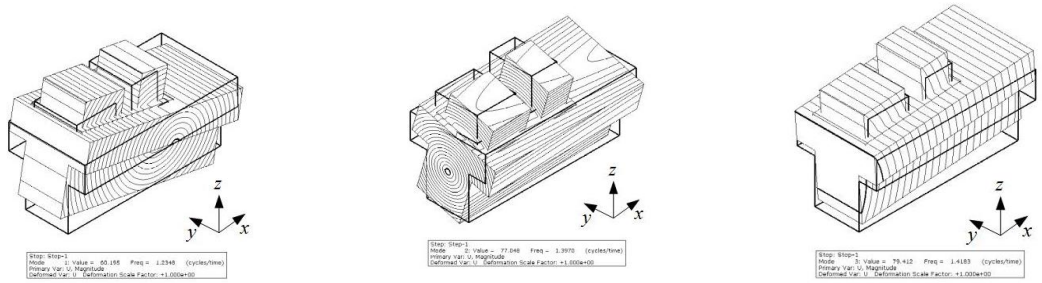

f_1 =1.235 Hz (Pitching) f_2 =1.396 Hz (Rolling) f_3 =1.42 Hz (Rocking.\)

Figure 7. *The first three eigen-modes of the system*

3.3. The real base isolation system: Sine-sweep test results

A sine-sweep vibration test for determination of first few fundamental frequencies was carried out to be sure that the system fundamental frequencies are sufficiently below the design requirement($f_i < 3Hz.$). The shaker excitation for the test is in vertical (z) direction. Two piezoelectric type accelerometers with a sensitivity of 500 mV/g are located on the top opposite corners of the isolation block diagonally to get the mode shapes and corresponding frequencies (See the
Figure 8). The sweep rates for sine sweep test was done for both 1 and 2 octaves/min from 1 to 10 Hz to figure out the effect of sweep rate. It was found that the sweep rate affects the amplitude but does not affect the resonant frequencies. A dummy load having 600 kg mass is placed at the top of shaker.

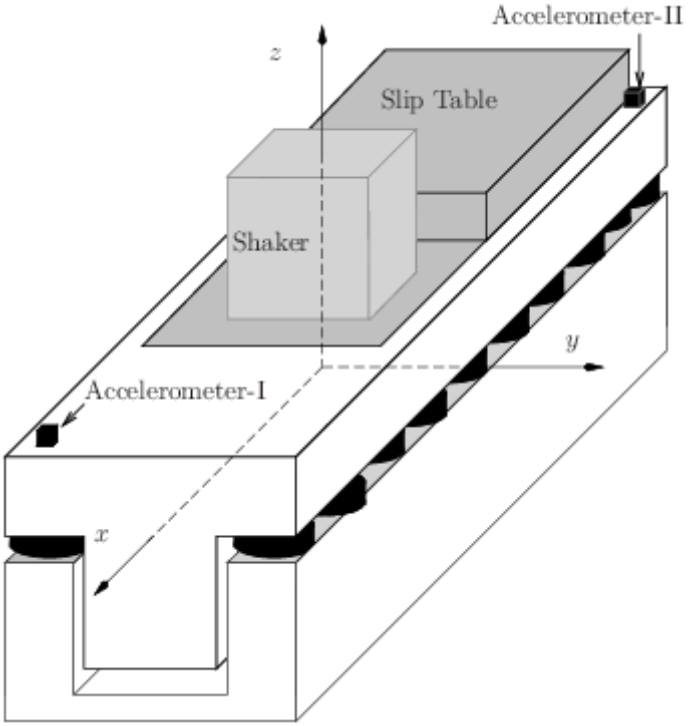

Figure 8. *Accelerometers for the sine-sweep test*

The accelerometer readings are plotted and they are shown in the Figure 9. The sweep-rate, damping and frequency range for the sine-sweep test affect the maximum amplitudes of the response. Sensitivity of the data acquisition system and accelerometers also affect the test results. Thus, capturing and determination exact resonance frequencies from the test results have some difficulties and uncertainties. However, the location of maximum amplitudes on the test graph agree well with the math and finite element model results. As can be seen on the graph on the Figure 9 the first interval for maximum amplitudes starts from 1.2 Hz and ends around 1.5 which is the range of the first three eigen-frequencies. The second interval for the maximum amplitudes is short and between 1.8 and 1.9 which corresponds to the 4*th* and 5*th* eigen-frequencies. Math and finite element results for second and third eigen-frequencies are close to each other and they are around 1.4 Hz. Similarly, the fourth and fifth frequencies are almost repeating and they are around 1.9 Hz.

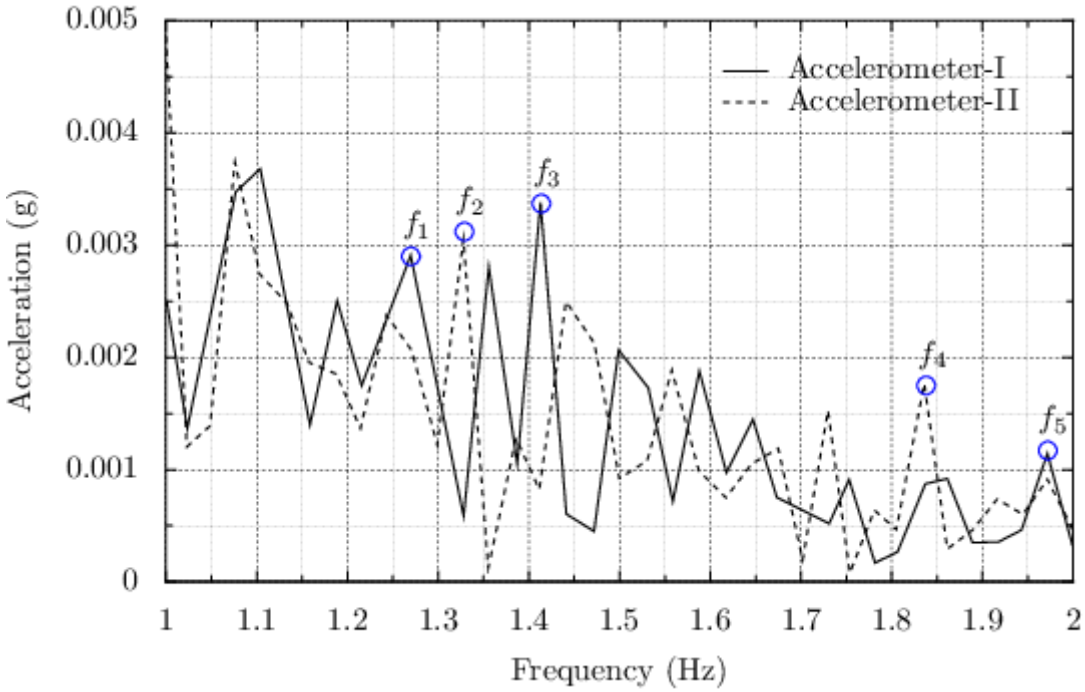

Figure 9. *The sine-sweep vibration test accelerometer reading records*

Eigen-modes of the system can be interpreted from the accelerometer readings, for example when the difference of the accelerometer amplitudes are maximum, then the pitching or rolling of the block occurs (See Figure 9). This is because of the placement of accelerometers at the opposite corners. The first mode, at 1.27 Hz, is pitching of the block, i.e. rotation around the y-axis. Similarly, the second mode, at 1.32 Hz, is rolling of the block, i.e. rotation around the x-axis. The third mode is the rocking around the slip table and is within the range of 1.36-142 Hz. The higher modes are mixed of translation, rocking, rolling and yawing. Thus, it is difficult to describe modes from the test with two accelerometers located at the corners only. The main purpose of the test was to ensure the rigid body modes are below the minimum excitation frequency of the test system. The test results have already satisfied the design criteria and no more tests to define mode shapes or any other parameters were needed.

The mode shapes based on the system coordinates is described in the Table 1. The table shows the test, the proposed math model and the finite element model results. The mode shapes are expressed in their dominant behavior in the Table 1.

Table 1. *Mode shapes and frequencies based on the test*

Mode		**Frequency (Hz).**			**Error %**	
No	**Shape**	**Test**	**Math Model**	**FE Model**	**Test-Math**	**Test-FE Model**
1	Pitching	1.27	1.233	1.235	2.76	-3.6
2	Rolling	1.32	1.36	1.397	-5.76	-1.3
3	Rocking	1.36-14	1.42	1.42	-2.9	0.5
4	Rocking	1.84	1.882	1,8921	-2.3	-2.8
5	Rocking	1.97	1.893	1.9361	-3.9	1.7
6	Pit. &Roll.	1.97	2.242	2.2730	-13.0	-15.4

The test is specifically designed to determine the rigid body frequencies with minimal number of accelerometers. The finite element model uses simplified and idealized boundary conditions and material properties. The math model is also based on the idealized boundary conditions and material properties. Thus, there is no bench-mark data to make comparison of the results. However, the results agree well with each other as shown in the Table 1. There are insignificant differences between the results. The design criteria requirement is absolute maximum differences between the design and actual test results must be less than 5 percent. As shown on the comparison table, all the frequencies found are within the requirement

limit except the sixth frequency. The minor differences between the test and math models can be attributed to some modeling simplifications, idealizations of the math and finite element models and some other factors. These are, not limited to, a) the simplifications in math and finite element models, such as point approximation of the actual wide supports as point supports and mass-less springs assumptions, b) the mass and mass distribution difference of the actual structure, the math and finite element models, c) imperfections in manufacturing of the isolation block and errors due to test measurements, etc.

4. CONCLUSION AND FUTURE STUDIES

In this study, the equation of motion for the dynamics analysis of vibration isolation system is derived by using the vector algebra. The formulation is based on coordinate system located at the center of mass of the system. The math model assumes that the isolation block is rigid body and springs supporting the block are massless. The static stiffness matrix for the system is derived by using rigid body motion of a massive block undergoing small deformations and supported by mutually placed elastic springs. The mass matrix is common mass matrix derived for rigid body dynamics. The system has 6 rigid body degree of freedom as generalized coordinates. The math model is applied to a real vibration isolation system manufactured for vibration testing of spacecraft and their subsystems. Ideal case for the system is perfect symmetry in the mass and spring distributions. In that case the mass and stiffness matrices become diagonal and the math model results in six uncoupled eigen-modes. Unsymmetrical springs cause distance between the mass and stiffness center of the system. This distance is defined as eccentricity and can be classified as 1-D, 2-D or 3-D depending upon the location of the eccentricity vector. A finite element model also is developed to confirm the model analysis results. The eigen-analysis results obtained from math model and finite element model are compared with the finite element and real test results. The results of the math model agree well with the test and finite element results. The math model can be used in design, analysis and test of the vibration isolation systems. The study can be extended to variety of related static and dynamic analysis of vibration isolation systems, such as analysis under dynamic excitation and loading.

CONFLICT OF INTEREST

The author declares that there is no conflict of interest regarding the publication of this paper.

REFERENCES

[1] Abaqus FEA software, Computer software https://www.3ds.com/products-services/simulia/products/abaqus/ 2017.
[2] J. Angeles, “On the Nature of the Cartesian Stiffness Matrix,” *Ingeniería mecánica, tecnología y desarrollo*, vol. 3, no. 5, pp. 163–170, 2010.
[3] J. Angeles, *Fundamentals of Robotic Mechanical Systems: Theory, Methods, and Algorithms*, 3rd ed. Springer International Publishing, 2013.
[4] B. Bachman, *Vibration Problems in Structures; Practical Guidelines*. Birkhauser Verlag Basel Boston Berlin, 1997.
[5] M/L Technical Bulletins, “Elastomer or Spring Isolators: Which Type to Use and When.” retrieved http://www.vibrodynamics.com/usa/bulletin.html 2017.
[6] J. Harry Himelblau and R. Sheldon, *Vibration of a Resiliently Supported Rigid Body*, 6th ed. McGraw-Hill, 2010, pp. 1–56.
[7] R. A. Ibrahim, “Recent advances in nonlinear passive vibration isolators,” *Journal of sound and vibration*, vol. 314, no. 3, pp. 371–452, 2008.
[8] W. D. Iwan, “The earthquake design and analysis of equipment isolation systems,” *Earthquake Engineering & Structural Dynamics*, vol. 6, no. 6, pp. 523–534, 1978.
[9] E. S. Leonard, “Generalized Matrix Method for the Design and Analysis of Vibration-Isolation Systems,” *The Journal of the Acoustical Society of America*, vol. 40, pp. 195–204, 1966.
[10] P. Madsen, “A Mathematical Approach to the Forced Vibrations of the Suspended Compressor Block,” in *International Compressor Engineering Conference*, 1972, no. Paper 52, pp. 326–329.
[11] S. R. Singiresu, *Mechanical Vibrations*, 5th ed. Prentice Hall, 2011.

[12] M. Stephen, "Analytical Modelling of Single and Two-Stage Vibration Isolation Systems," in *Proceedings of the Annual Conference of the Australian Acoustical Society Acoustics 2011: Breaking New Ground*, 2011, p. 116.
[13] Cfm-Schiller website, "Steel Spring Isolators - Type SSI." http://www.cfm-schiller.de/index.php?zeige_rubrik=15&dbase=produktdetails, 2017.
[14] J. Z. Yongjun Jin and X. Guan, "Theroretical Calculation and Experimental Analysis of the Rigid Body Modes of Powertrain Mounting System," *WSEAS Transactions on Applied and Theoretical Mechanics*, vol. 8, no. 3, pp. 193–201, Jul. 2013.